Temperature dependence of anomalous luminescence decay: Theory and experiment

E. Mihóková,[1,*] L. S. Schulman,[2] M. Nikl,[1] B. Gaveau,[3] K. Polák,[1] K. Nitsch,[1] and D. Zimmerman[2]
[1]*Institute of Physics, Academy of Sciences of the Czech Republic, Cukrovarnická 10, 162 53 Prague 6, Czech Republic*
[2]*Physics Department, Clarkson University, Potsdam, New York 13699-5820*
[3]*Université Paris 6, Géométrie des Équations aux Dérivées Partielles et Physique Mathématique, Case Courrier 172, 4 Place Jussieu, 75252 Paris Cédex 05, France*
(Received 30 August 2001; Revised 17 July 2002; published 3 October 2002)

The anomalous decay of slow emission in impurity-doped alkali halides is studied both experimentally and theoretically. Experiments systematically examine the decay of luminescence in Pb^{2+}-doped KBr for temperatures from 6 to 110 K and for times from 40 μs to 40 ms. Theoretical methods, previously used to explain the anomaly at low temperature, are extended to deal with phonon-induced transitions and other high-temperature phenomena. The significant ansatz of this and the previous work is slow (ms scale) relaxation of the lattice. This ansatz continues to allow successful theoretical fitting of the data.

DOI: 10.1103/PhysRevB.66.155102 PACS number(s): 31.70.Hq, 78.55.Fv, 83.85.Ns, 71.55.−i

I. INTRODUCTION

In previous work[1,2] we proposed a model to explain an anomaly in the slow-component decay of emission in doped alkali halides. The doping is by heavy ions with an ns^2 ground-state electronic configuration; for reviews, see, e.g., Refs. 3 and 4. Nonexponential decay of emission under *A*-band excitation was experimentally observed in Pb^{2+}- and Tl^+-doped potassium halides[5–9] with fcc crystal lattices. This phenomenon is not confined to the systems mentioned and is observed for alkali halides with bcc lattice structure as well.[10] Based on the purity of the samples, the preparation technique, and the reproducibility of the results, we believe that the particular character of the decay is an intrinsic property of the emission centers in alkali halide crystals. These features are discussed below as well as in Ref. 1. Besides reporting new and extensive experimental results that in particular reconfirm the anomaly, the present paper is concerned with the introduction of further theoretical methods. This allows us to extend our previous explanation of the anomaly to considerably higher temperatures, basically until the nonexponential decay nearly disappears.

The emitting unit of the system is a quasimolecule consisting of the central impurity ion and its nearest neighbors. For an fcc lattice this structure has the form AX_6^{i-} [$A=Tl^+$ (Pb^{2+}); $X=$Cl, Br, I; $i=5$ (4)] and possesses O_h symmetry. The lowest relaxed excited state of this unit consists of two levels, the so-called *radiative* and *metastable* levels. These have significantly different lifetimes, as determined by selection rules. This level scheme explains the presence of two components in the emission decay—fast ($\sim$ns) and slow ($\sim$ms)—and is now generally accepted (see, e.g., Refs. 3 and 11). It is a consequence of the Jahn-Teller and spin-orbit interactions.

Our model,[1] which explains the nonexponential character of the slow-component decay, is based on the assumption that the lattice relaxes on the same time scale as the slow-component decay. This relaxation is a response to the Jahn-Teller local distortion of the luminescence centers. In the framework of our model we obtained successful fits to the experimental data at liquid He temperatures for K*X*:*A* (*X* =Cl, Br, I; $A=Tl^+$, Pb^{2+}) systems.[2] The dependence of the fitting parameters on lattice and impurity allows systematic physical interpretation. This model has not yet been used to address the behavior of the decay at higher temperatures. Experimental results in Ref. 5 showed that with increasing temperature the anomalous (nonexponential) part of the slow decay gradually becomes less evident and vanishes completely around 150 K.

As indicated, in the present work we provide experimental data studying the temperature dependence of the slow decay for KBr:Pb^{2+}. Moreover, we extend the theoretical model to higher temperatures. We show the calculated fits of the experimental data in a wide temperature range, 6–110 K, and discuss the temperature dependence of the parameters of our model. An important issue, discussed to some extent in Ref. 2 and more fully in Ref. 12, is the explanation of the extremely slow relaxation (from a natural scale of picoseconds to one of milliseconds) of the lattice.[13]

II. EXPERIMENTAL METHODS

Single crystals of KBr:Pb^{2+} were grown by the Bridgman method using a quartz ampoule. A low concentration of $PbBr_2$ (0.005 mol %) was used in the raw material to prevent Pb^{2+} ion clustering. In the preparation procedure multiple zone melting and special treatment in a halide atmosphere were used to suppress unwanted cationic and anionic impurities.[14] Prior to the luminescence measurement the sample was heated at about 500 °C for 1 h in vacuum and then rapidly quenched to room temperature to destroy possible Pb^{2+}-based clustering. These measures were taken to minimize the effect of defects and to ensure that each Pb ion enjoyed the same environment as any other and could be considered isolated, thereby eliminating certain suggested explanations of the decay anomaly (e.g., a statistical averaging over inequivalent centers, as could be the case in glasses[15]).

The decay kinetics of Pb^{2+} emission at 360 nm was measured on a spectrofluorometer 199S (Edinburgh Instrument) using an Oxford helium flow cryostat (see also Ref. 7). Excitation was performed using a xenon-microsecond

flashlamp. The luminescence signal was detected by a multichannel analyzer in the scaling regime. Two time resolutions, 10 μs and 100 μs per channel, were used so as to obtain sufficient information for all time regimes of interest.

III. DECAY THEORY, INCLUDING TEMPERATURE DEPENDENCE

A. Preliminaries and notation

The theoretical framework is the same as in our previous work.[1,2] However, because those papers were concerned with ''zero'' temperature we were able to employ a purely Hamiltonian formalism; the only decay process was through coupling to the electromagnetic field, a process that did not destroy the coherence of the undecayed portion of the wave function. In the present paper we introduce a formalism for handling the ''finite'' temperature problem. Finite temperature effects take two forms: the availability of phonons that can induce transitions between electronic states, and changes in lattice relaxation properties. We will recall just enough of our previous work to explain the density-matrix technique introduced here.

In the experiment the Pb is excited by a UV pulse and goes to one of two excited states, a radiative level or a metastable level. For details, see Refs. 1 and 2. These states are effectively electronic states of the idealized molecular complex which consists of the central Pb impurity ion and its six neighbors. The term ''idealized'' refers to the exclusion of interaction with other ions of the lattice.

The lattice interaction has two effects. First it prevents the collective coordinate of the molecular-complex nuclei (to be called ''*R*'') from relaxing to its preferred value. As a consequence the splitting between the two electronic states is less than it would be in the absence of the lattice's constraining influence. Second, the lattice interaction introduces a coupling between the molecular electronic levels. Our effective two-state Hamiltonian, which includes these two features, as well as a finite lifetime against radiative decay, is[1,2]

$$H=\begin{pmatrix} E(R)-\frac{i}{2}\hbar\gamma_f & \alpha(R) \\ \alpha(R) & -\frac{i}{2}\hbar\gamma_s \end{pmatrix}. \tag{1}$$

$E(R)$ is the energy difference between levels, imaginary parts of the energies give the radiative decay, and $\alpha(R)$ is the coupling between levels. In practice the ''fast'' and ''slow'' decay rates differ by a factor of about 10^5. As the collective coordinate, *R*, increases, the energy difference approaches its pure molecular value and the coupling, α, approaches zero.

As a function of time, we take $R(t)$ of the form

$$R(t)=R_0+(R_\infty-R_0)[1-f(t)], \tag{2}$$

with $f(0)=1$ and $f(\infty)=0$. We here consider two possibilities,

$$f_{\exp}(t)=\exp(-\Gamma t), \tag{3}$$

$$f_{\text{power}}(t)=(1+\Gamma t)^{-3/2}. \tag{4}$$

The first represents a typical relaxation response, the second is based on a phonon diffusion model.[16] Using one or another form of $R(t)$, the energy difference between the levels and the variation of coupling strength are

$$E=E_0+(E_f-E_0)[1-f(t)], \tag{5}$$

$$\alpha=\alpha_0+(\alpha_f-\alpha_0)[1-f(t)], \tag{6}$$

where (E_0,α_0) and (E_f,α_f) are the initial and asymptotic values, respectively. (α_f will always be taken to be 0.)

It is convenient to rewrite *H* in terms of the Pauli spin matrices. In this representation

$$H=H_0-i\frac{\hbar}{2}g, \tag{7}$$

with H_0 and g real Hermitian matrices

$$H_0=\frac{E}{2}\sigma_3+\alpha\sigma_1$$

and

$$g=\frac{1}{2}(\gamma_f+\gamma_s)\sigma_0+\frac{1}{2}(\gamma_f-\gamma_s)\sigma_3. \tag{8}$$

In H_0 the energy has been shifted by $E/2$ relative to the form in Eq. (1), which makes no dynamical difference, and $\sigma_0 \equiv \mathbf{1}$ is the 2×2 identity matrix.

B. Density-matrix formalism

To deal with the effect of temperature we go to a density-matrix formalism. This could have been done in our previous low-temperature work[1,2] to treat radiative decay, but using Hamiltonian dynamics with an imaginary energy accomplished this more simply.

The density matrix can be written in extended Bloch form,[17]

$$\rho=\sum_{\alpha=0}^{3} r_\alpha\sigma_\alpha=r_0\mathbf{1}+\vec{r}\cdot\vec{\sigma}. \tag{9}$$

To invert Eq. (9) we use $r_\alpha=\frac{1}{2}\,\mathrm{Tr}\,\sigma_\alpha\rho$. Our Hamiltonian, Eq. (1) [or Eq. (7)], has an anti-Hermitian part, so that in place of the usual $i\hbar\dot{\rho}=[H,\rho]$, the density-matrix equation, at zero temperature, takes the form

$$i\hbar\dot{\rho}=H\rho-\rho H^\dagger=[H_0,\rho]-i\frac{\hbar}{2}\{g,\rho\}, \tag{10}$$

with curly brackets indicating the anticommutator.

We next include the effects of thermal phonons at nonzero temperatures. Thermal coupling can induce nonradiative transitions between the levels. The change in ρ due to these transitions, when in the presence of *n* phonons of energy *E*, contributes the following term to Eq. (10):

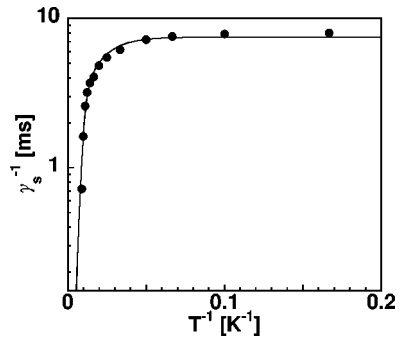

FIG. 1. Temperature dependence of the asymptotic slow-level lifetimes, $1/\gamma_s$, used in our fits. Circles are the data derived from late-time luminescence decay, while the solid line is a fit using procedures described in Ref. 6 (see also text).

$$i\hbar\dot{\rho}_{\text{phonon}} = i\hbar K \begin{pmatrix} n\rho_{22} - (n+1)\rho_{11} & -D\left(n+\frac{1}{2}\right)\rho_{12} \\ -D\left(n+\frac{1}{2}\right)\rho_{21} & -n\rho_{22} + (n+1)\rho_{11} \end{pmatrix}. \tag{11}$$

The quantity K is an asymptotic low-temperature transition rate, since at sufficiently low temperature "n" is effectively zero. It will be phenomenologically determined for our data fits. The number D governs the decoherence. For phonon-state coupling of the spin-boson form, $D=1$, and we adopt this value in our numerical work.

For the phonon number, n, we take the expected number of phonons of energy E to be found at temperature T. This is given by the Boltzmann factor

$$n = \frac{1}{\exp(E/kT)-1}. \tag{12}$$

The full equation for ρ is

$$i\hbar\dot{\rho} = [H_0,\rho] - i\frac{\hbar}{2}\{g,\rho\} + i\hbar\dot{\rho}_{\text{phonon}}. \tag{13}$$

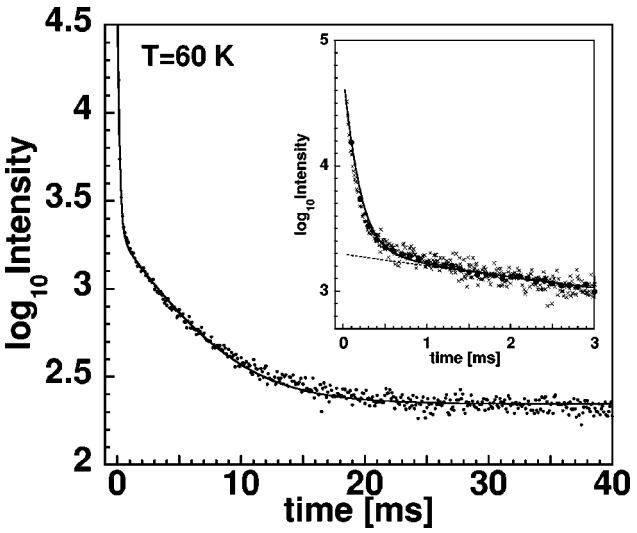

FIG. 2. Example of luminescence decay in the entire time range 0–40 ms for the temperature $T=60$ K. Points are experimental data. The solid curve is the fit obtained using our model with exponential lattice relaxation [Eq. (3)]. The values of the calculated curve are normalized to the experimental data. The dashed curve represents an exponential fit to the late-arriving data. The temperature-independent parameters used are $\gamma_f = 4\times10^4$ ms^{-1}, $E_f = 60$ meV, and $K = 280$ ms^{-1}. The temperature-dependent parameters are $E_0 = 20.9$ meV, $\Gamma = 0.848$ ms^{-1}, and $\alpha_0 = 0.0281$ meV. The inset focuses on the period 0–3 ms. Crosses are the experimental data measured in the range of times 0–5 ms. Solid circles are the experimental data measured in the range of times 0–40 ms.

This is a linear equation for the four components of ρ. It is convenient to express Eq. (13) in terms of the components of the extended Bloch form, Eq. (9), by defining a column vector r with components r_0, r_1, r_2, and r_3. This vector satisfies

$$\dot{r} = Wr, \tag{14}$$

with

$$W = \begin{pmatrix} -\gamma_0 & 0 & 0 & -\gamma_3 \\ 0 & -\gamma_0 - Kn'D & -2w & 0 \\ 0 & 2w & -\gamma_0 - Kn'D & -2a \\ -\gamma_3 - K & 0 & 2a & -\gamma_0 - 2Kn' \end{pmatrix}. \tag{15}$$

In Eq. (15) we use the notation $a \equiv \alpha/\hbar$, $w \equiv E/2\hbar$, $\gamma_0 \equiv \frac{1}{2}(\gamma_f + \gamma_s)$, $\gamma_3 \equiv \frac{1}{2}(\gamma_f - \gamma_s)$, and $n' = n + \frac{1}{2}$.

Our results are based on numerical integration of Eq. (14). There is a potential hazard here in that the nonzero components of W differ from one another by factors as large as 10^9. Exponentiation of W on MATLAB (which retains 14 to 16 significant digits) was found to be accurate by checking against 50 digit accuracy with other computational software (MATLAB uses a Padé approximant method of exponentiation).

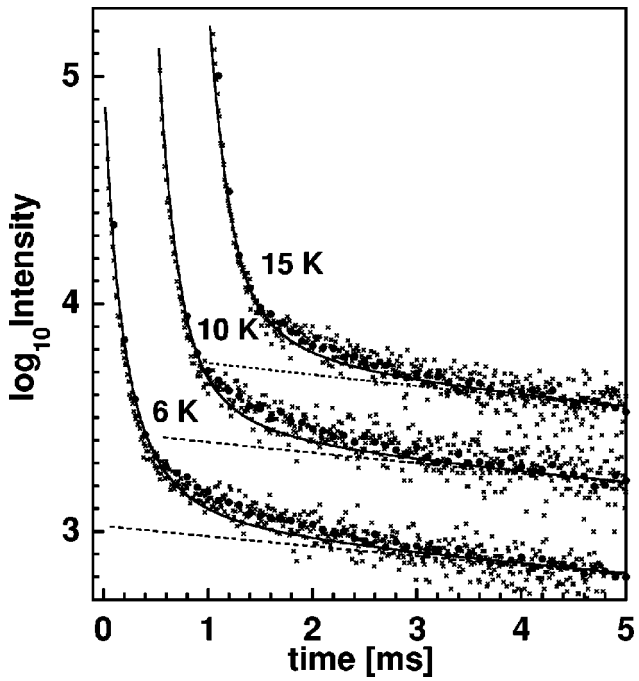

FIG. 3. Decay curves of KBr:Pb^{2+} for temperatures 6 K, 10 K, and 15 K. Crosses are the experimental data measured in the time interval 0–5 ms. Circles are the experimental data measured in the interval 0–40 ms. The solid curve is the fit obtained using our model with exponential lattice relaxation [Eq. (3)], with the values of the calculated curve normalized to the experimental data. The dashed curve represents an exponential fit to the late-arriving data. The temperature-dependent parameters are given in Table I. The axes correspond to the temperature 6 K. For better display the data for 10 K are shifted 0.5 units to the right on the time axis and 0.4 upward on the log-intensity axis. The respective shifts for 15 K are (1, 0.8).

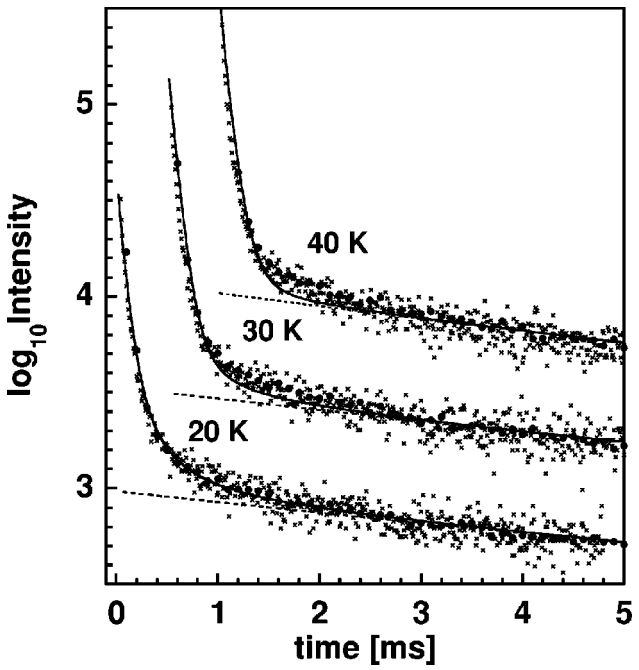

FIG. 4. Decay curves of KBr:Pb^{2+} for temperatures 20 K, 30 K, and 40 K. The meaning of the symbols is the same as in Fig. 3. The temperature-dependent parameters used for the fit are given in Table I. The axes correspond to the temperature 20 K. Once again, for better display the data for other temperatures are shifted. The respective temperatures, time shifts, and log-intensity shifts are given by (30 K, 0.5, 0.4) and (40 K, 1, 1).

IV. RESULTS AND DISCUSSION

Figure 1 displays the temperature dependence of the slow-component decay lifetimes. The values (circles) were obtained by fitting the decay curve at late times, when the decay is well described by an exponential. The solid line in Fig. 1 will be explained below. Figure 2 shows an example (at 60 K) of both the full decay pattern and (in the inset) the first few ms. At large times the curve is approximately an exponential plus constant background. To highlight the deviation from this behavior we have put a dashed line in the inset. This line is the continuation to small times of the exponential that matches the data at large times. Figures 3–6 present the experimental data together with the fits of those data calculated by our model (and the dashed line has the same significance). The experimental data were taken on two time scales: *crosses* represent the data obtained in a measurement performed in the time interval 0–5 ms to get the initial (nonexponential) part of the decay curve in detail; *circles* represent the data obtained from a measurement performed in the time interval 0–40 ms to get the complete decay curve. Only the first 3–5 ms of data are shown, since this is the most difficult part of the fit. In these figures we only present fits based on the exponential model of lattice relaxation [Eq. (3)] as the fits based on the phonon diffusion model [Eq. (4)] are qualitatively similar.

Although many parameters enter the fitting procedure, several of them are fixed by other considerations. The entire list of parameters is E_0, E_f, α_0, Γ, and K and the electromagnetic decay rates. Some of these have a temperature dependence and some do not. The fast electromagnetic decay rate is temperature independent in the range of temperatures here studied. Its value, 4×10^4 ms^{-1}, is taken from early-time measurements, well before the phenomenon we study appears. The slow electromagnetic decay rate varies significantly with temperature and, as indicated above, was determined for each temperature by fitting the late-time data (see Fig. 1). The temperature dependence of these late-time decay rates in turn allowed us to evaluate $E_f=60$ meV and $K=280$ ms^{-1}, by means of a density-matrix formalism much like that in Eqs. (11) and (13), except considerably simpler because of the constancy of the energy and the absence of lattice-quasimolecule coupling ("α"). This is the procedure used, for example, in Ref. 6 and described in detail there. This fit is shown as the solid line in Fig. 1. The parameters E_f and K were therefore taken *without* temperature dependence.

As a result of these considerations, the only parameters to be fit by our model (at each temperature) were E_0, the initial energy split, α_0, the initial coupling, and Γ, the lattice relaxation rate, all of which are expected to have significant variation (especially Γ). Note also that part of the temperature dependence in E_0 and α_0 arises from the variation of lattice

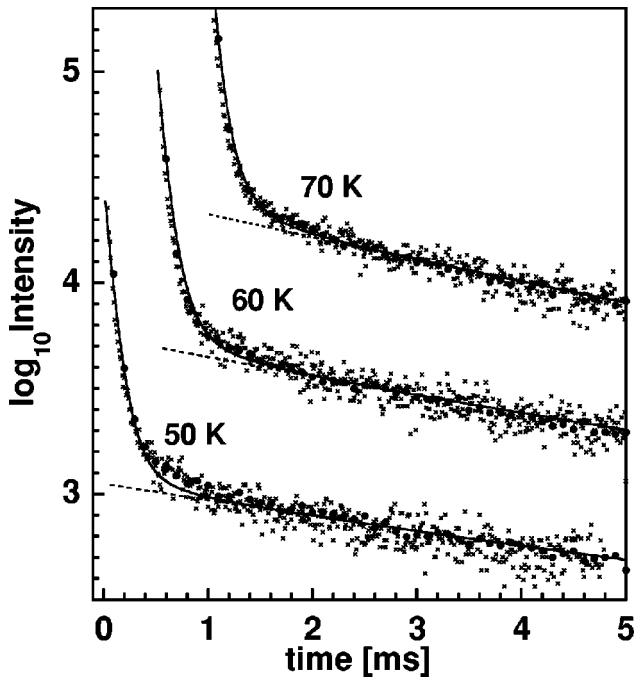

FIG. 5. Decay curves of KBr:Pb^{2+} for temperatures 50 K, 60 K, and 70 K. The meaning of the symbols is the same as in Fig. 3. The temperature-dependent parameters used for the fit are given in Table I. The axes correspond to the temperature 50 K. Again, for better display the data for other temperatures are shifted. The respective temperatures, time shifts, and log-intensity shifts are given by (60 K, 0.5, 0.4) and (70 K, 1, 1).

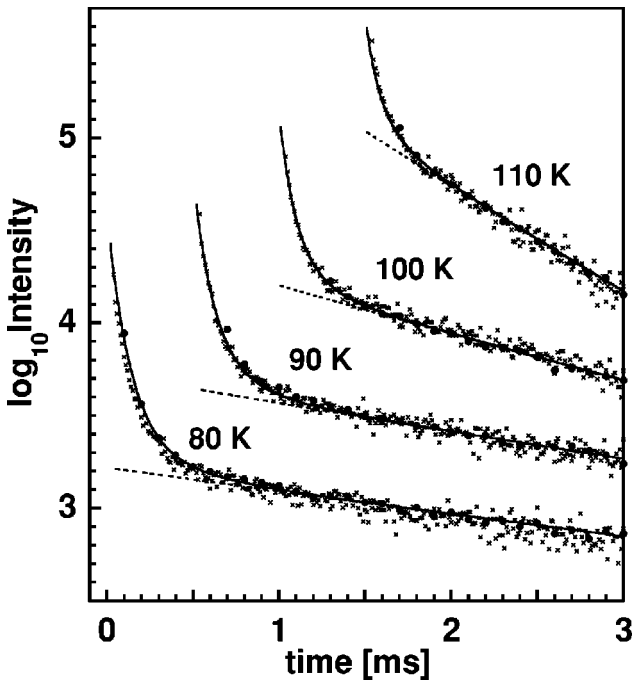

FIG. 6. Decay curves of KBr:Pb^{2+} for temperatures 80 K, 90 K, 100 K, and 110 K. The meaning of the symbols is the same as in Fig. 3. The temperature-dependent parameters used for the fit are given in Table I. The axes correspond to the temperature 80 K. Again, for better display the data for other temperatures are shifted. The respective temperatures, time shifts, and log-intensity shifts are given by (90 K, 0.5, 0.4), (100 K, 1, 0.7), and (110 K, 1.5, 1.4).

relaxation, in that the time referred to as ''initial'' is effectively that of the first data point used in the fit (usually at 40 μs). This is discussed below. The results of these fits are shown in Fig. 7 and Table I. Note that the figure and table include information on both relaxation patterns, exponential and power law, although we have only shown detailed fits at each temperature for exponential relaxation.

Other patterns of relaxation, besides exponential and power law, could also have been used, opening the door to what could effectively be considered an infinity of fitting parameters. Quite likely fine tuning of the function *f* appearing in Eq. (2) could have led to even better fits than those we have obtained; nevertheless, we felt that providing substantial agreement between theory and experiment while sticking to generic relaxation behavior would better make our point.

We conclude this section with a discussion of additional points of relevance to our model and its experimental status. In the theoretical treatment we have the capability to distinguish contributions to slow emission from the metastable and the radiative levels. There is a good possibility that the radiation from these levels can be distinguished experimentally on the basis of polarization. At present, the intensities are not sufficient for us to make this measurement with our equipment, but should that become possible it could serve as a further test of the theory. Another point of interest is the absence of decay anomalies under excitation in the *C* band. This was noted in earlier work,[5] although the purpose of the *C*-band excitation studies at that time was to check the accuracy of the apparatus. In any case, the absence of anomalies when excitation occurs via the *C* band can be understood in terms the much higher amount of energy (an eV) that is dissipated locally, thereby effectively creating a local high-temperature system. As we have seen in the results reported in the present paper, such heating leads to suppression of the anomaly.

V. CONCLUSIONS

The main conclusion of our work is that the slow lattice relaxation model, used to explain anomalous decay at low temperatures (4–6 K), continues to work—with appropriate extension—at much higher temperatures, essentially until the anomalous decay phenomenon is no longer significant. This conclusion is reached by successful fits of the experimental

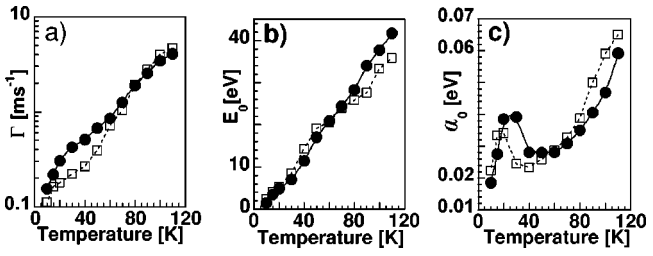

FIG. 7. Temperature dependence of the parameters Γ, E_0, and α_0. Circles represent the data obtained for the exponential lattice relaxation [Eq. (3)], while squares correspond to diffusion-related lattice relaxation [Eq. (4)].

TABLE I. Parameter values for KBr:Pb^{2+}.

		Exponential relaxation			Power-law relaxation		
T (K)	$1/\gamma_s$ (ms)	Γ (ms^{-1})	E_0 (meV)	α_0 (10^{-2} meV)	Γ (ms^{-1})	E_0 (meV)	α_0 (10^{-2} meV)
6	8.0	0.098	0.965	1.29	0.061	0.994	1.17
10	7.9	0.153	1.42	1.85	0.111	2.40	2.24
15	7.6	0.217	3.48	2.74	0.162	4.14	3.35
20	7.2	0.304	4.87	3.85	0.178	5.28	3.41
30	6.2	0.421	6.96	3.91	0.220	8.46	2.45
40	5.5	0.507	11.37	2.80	0.264	14.32	2.33
50	4.8	0.667	16.98	2.79	0.392	19.10	2.58
60	4.1	0.848	20.86	2.81	0.715	20.64	2.86
70	3.7	1.25	24.37	3.07	1.03	23.96	3.27
80	3.2	1.87	28.28	3.49	1.93	25.80	3.87
90	2.6	2.55	33.95	4.04	2.77	27.58	5.00
100	1.6	3.40	37.63	4.68	4.00	33.31	5.90
110	0.7	4.04	41.66	5.91	4.68	35.77	6.50

data using parameters with reasonable temperature dependence. We point out that besides improvements in the quality of the crystal, the present data are recorded at significantly earlier times than in our previous work. As a result, the anomalous regime is probed more intensively, presenting a far greater challenge for the model. Thus it was not at all obvious that the slow relaxation hypothesis would survive both the theoretical and experimental extensions of its applicability.

For some of our parameters, we needed (and expected) no temperature dependence, namely, the phonon relaxation parameter (''K'') and the asymptotic (relaxed lattice) energy splitting (''E_f'').

On the other hand, for the parameter Γ, the lattice relaxation rate, there is a strong and expected temperature dependence. Surely the fact that the lattice relaxes more rapidly as it warms is no surprise. From 6 K to 110 K this relaxation speeds up by a factor of about 50 and shows an approximately exponential increase with temperature. This is true for both patterns of lattice relaxation, exponential and power law [see Fig. 7(a)].

For E_0 there is significant variation (nearly linear), which we also do not find surprising. The splitting of the lowest excited state in the tetragonal minima into a radiative doublet and a metastable singlet is caused by spin-lattice relaxation.[11] If we accept this ''Condon-violated'' mechanism for our system, the splitting, E, between the radiative and metastable levels, could be temperature dependent, since the state of the lattice (including the immediate neighbors of the impurity) is itself temperature dependent. A second and related aspect is that we observe the emission after some delay (our initial observation is at a fixed time, generally 40 μs after the initial flash) which means that the lattice is already partially relaxed. Since the speed of lattice relaxation (the parameter Γ) increases with temperature this implies that the effective E_0 changes.

The quantity α_0 presents more complex behavior. Inasmuch as it represents a coupling to the lattice, it is possible that interesting physics lurks in its peak around 20 K, but we offer no specific suggestion, pending a better understanding of the lattice-quasimolecule interaction. On the other hand, one should note that the changes in α_0 in the region around the peak (10–30 K) and throughout its range are small in absolute scale (a factor of 3, rather than $\sim$50 for the other parameters) which suggests lesser physical significance.

These conclusions have been reached based on measurements, also reported here, in which the crystal-growth technique, the purity of the sample, and other experimental precautions all guarantee that the anomalous decay is an intrinsic property of the material and not due to defects or statistical averages.

ACKNOWLEDGMENTS

This work was supported by United States National Science Foundation Grants Nos. PHY 9721459 and PHY 0099471 and by the Czech Grants Nos. ME382 and AVOZ1-010-914.

*Email address: mihokova@fzu.cz

[1] B. Gaveau, E. Mihóková, M. Nikl, K. Polák, and L.S. Schulman, Phys. Rev. B **58**, 6938 (1998).
[2] B. Gaveau, E. Mihóková, M. Nikl, K. Polák, and L.S. Schulman, J. Lumin. **92**, 311 (2001).
[3] A. Ranfagni, D. Mugnai, M. Bacci, G. Viliani, and M.P. Fontana, Adv. Phys. **32**, 823 (1983).
[4] P.W.M. Jacobs, J. Phys. Chem. Solids **52**, 35 (1991).
[5] K. Polák, M. Nikl, and E. Mihóková, J. Lumin. **54**, 189 (1992).
[6] J. Hlinka, E. Mihóková, and M. Nikl, Phys. Status Solidi B **166**, 503 (1991).
[7] J. Hlinka, E. Mihóková, M. Nikl, K. Polák, and J. Rosa, Phys. Status Solidi B **175**, 523 (1993).

[8] E. Mihóková, M. Nikl, K. Polák, and K. Nitsch, J. Phys.: Condens. Matter **6**, 293 (1994).
[9] M. Nikl (unpublished).
[10] M. Nikl, J. Hlinka, E. Mihóková, K. Polák, P. Fabeni, and G.P. Pazzi, Philos. Mag. B **67**, 627 (1993).
[11] V.V. Hiznyakov and N.N. Kristoffel, in *The Dynamical Jahn-Teller Effect in Localized Systems*, edited by Yu.E. Perlin and M. Wagner (Elsevier, Amsterdam, 1984), Chap. 9, p. 383.
[12] L.S. Schulman, E. Mihokova, A. Scardicchio, P. Facchi, M. Nikl, K. Polak, and B. Gaveau, Phys. Rev. Lett. **88**, 224101 (2002).
[13] Other slowed processes also occur in doped alkali halides and related materials. Often they depend on the weakness of the spin-lattice interaction, a property that lies behind the slow decay of the metastable level in $KBr:Pb^{2+}$ as well as other extremely slow relaxation phenomena. See, for example, A. Tannús, R.A. Carvalho, M.C. Terrile, and H. Panepucci, Phys. Rev. B **51**, 890 (1995).
[14] K. Nitsch, V. Hamplová, M. Nikl, K. Polḱ, and M. Rodová, Chem. Phys. Lett. **258**, 518 (1996).
[15] M. Martini, F. Meinardi, A. Vedda, I. Dafinei, P. Lecoq, and M. Nikl, Nucl. Instrum. Methods Phys. Res. B **116**, 116 (1996).
[16] A third possibility for modeling the lattice is that it relaxes suddenly, waiting perhaps for one or several barrier penetrationlike events. This possibility is discussed in Ref. 2, but was found to give inferior fits to the data.
[17] R. Loudon, *The Quantum Theory of Light*, 2nd ed. (Clarendon Press, Oxford, 1983).